Data Continuity of Earth Observing 1 (EO-1) Advanced Land Imager (ALI) and Landsat TM and ETM+

Ross Bryant, M. Susan Moran, Stephen A. McElroy, Chandra Holifield, Kurtis J. Thome, Tomoaki Miura, *Member, IEEE*, and Stuart F. Biggar

***Abstract*—The National Aeronautics and Space Administration (NASA) Landsat program has been dedicated to sustaining data continuity over the 20-year period during which Landsat Thematic Mapper (TM) and Enhanced TM Plus (ETM+) sensors have been acquiring images of the earth's surface. In 2000, NASA launched the Earth Observing-1 (EO-1) Advanced Land Imager (ALI) to test new technology that could improve the TM/ETM+ sensor series, yet ensure Landsat data continuity. The study reported here quantified the continuity of satellite-retrieved surface reflectance (ρ) for the three most recent Landsat sensors (Landsat-4 TM, Landsat-5 TM, and Landsat-7 ETM+) and the EO-1 ALI sensor. The study was based on ground-data verification and, in the case of the ETM+ to ALI comparison, coincident image analysis. Reflectance retrieved from all four sensors showed good correlation with ground-measured reflectance, and the sensor-to-sensor data continuity was excellent for all sensors and all bands. A qualitative analysis of the new ALI spectral bands (4p: 0.845–0.890 μm and 5p: 1.20–1.30 μm) showed that ALI band 5p provided information that was different from that provided by the ETM+/ALI shortwave infrared bands 5 and 7 for agricultural targets and that ALI band 4p has the advantage over the existing ETM+ near-infrared (NIR) band 4 and ALI NIR band 4 of being relatively insensitive to water vapor absorption. The basic conclusion of this study is that the four sensors can provide excellent data continuity for temporal studies of natural resources. Furthermore, the new technologies put forward by the EO-1 ALI sensor have had no apparent effect on data continuity and should be considered for the upcoming Landsat-8 sensor payload.**

***Index Terms*—Advanced Land Imager (ALI), data continuity, Earth Observing 1 (EO-1), Landsat Thematic Mapper 4 (TM4), Landsat Thematic Mapper 5 (TM5), Landsat Enhanced Thematic Mapper Plus (ETM+), remote sensing.**

I. Introduction

THE DATA from the National Aeronautics and Space Administration (NASA) Landsat program constitute the longest record of the earth's surface as seen from space. Landsat-1 was launched in 1972 with the Multi-Spectral Scanner (MSS), which was specifically designed for land remote sensing. This sensor proved so valuable that it was used with four subsequent Landsat missions. In 1982, Landsat-4 was launched with two sensors, MSS and a new sensor called the Thematic Mapper (TM), which had significant improvements in spatial resolution, as well as additional bands. The same payload was launched on Landsat-5 in 1984. Landsat-6 was launched in 1993 but failed to reach orbit. Landsat-7 was launched in 1999 with an improved TM sensor called the Enhanced Thematic Mapper (ETM+). ETM+ duplicated the TM technology but provided finer spatial resolution for the thermal sensor (60 m) and a new panchromatic band at 15-m resolution. The Advanced Land Imager (ALI) was launched in 2000 on the Earth Observing 1 (EO-1) satellite to test new technology that could be used for sensors aboard the next Landsat platform, Landsat-8. Compared to ETM+, ALI provides a greater SNR, a pushbroom sensor, greater quantization, and additional spectral bands with significant reduction in size, mass, and power [2].

As technology evolved, newer Landsat sensors were modified slightly, while keeping in mind the importance of historical data continuity. There is a keen interest in documenting data continuity over the different Landsat sensors. At least two studies comparing Landsat-4 TM and Landsat-5 TM sensors were performed when they were both operational. Metzler and Malila [3] found that Landsat-4 TM radiances were within ±10% of Landsat-5 TM radiances. Radiances in bands 2 and 5 had the greatest discrepancy with reduced radiances of 11% and 13%, respectively. Price [6] found very similar results with his comparison of Landsat-4 and Landsat-5 sensors. Subsequent work comparing Landsat-5 TM and Landsat-7 ETM+ yielded even better results. Vogelmann *et al.* [9] reported high band-to-band correlations for Landsat-5 TM and Landsat-7 ETM+ for the same targets in coincident scenes, ranging from $r^2 = 0.987$ in band 1 to $r^2 = 0.999$ in bands 4, 5, and 7. Vogelmann *et al.* [10] compared NDVI values with coincident Landsat-5 TM and Landsat-7 ETM+ scenes in Nebraska and found them essentially the same. He also subjected both scenes to a land classification scheme and obtained similar results.

This study attempts to quantify data continuity for the three most recent Landsat sensors and the EO-1 ALI sensor through ground data verification, and in the case of the ETM+ ALI comparison, coincident image analysis. We used the REL approach [4] for the comparison of Landsat-4 TM and Landsat-5 TM sensors, whereas for the other sensor compar-

Manuscript received July 19, 2002; revised February 20, 2003. This work was supported by the National Aeronautics and Space Administration (NASA) Earth Observing 1 (EO-1) Validation Team under Grant S-10217-X and by EO-1 Project Leader S. Ungar. This work built upon previous projects funded by the NASA Landsat-7 Science Team under Grant S-41396-F, with support from Landsat-7 Project Leader D. Williams.

R. Bryant, M. S. Moran, S. A. McElroy, and C. D. Holifield are with the U.S. Department of Agriculture, Agriculture Research Service, Southwest Watershed Research Center, Tucson, AZ 85719 USA.

K. J. Thome and S. F. Biggar are with the Optical Sciences Center, University of Arizona, Tucson, AZ 85721 USA.

T. Miura is with the Department of Soil, Water, and Environmental Science, University of Arizona, Tucson, AZ 85721 USA.

Digital Object Identifier 10.1109/TGRS.2003.813213

TABLE I
DATES FOR IMAGE ANALYSIS OF LANDSAT-4 AND LANDSAT-5 SENSORS AT MARICOPA

Date	DOY	Sensor
5/31/1989	151	Landsat 5 TM
6/16/1989	167	Landsat 5 TM
6/25/1989	175	Landsat 4 TM
7/2/1989	183	Landsat 5 TM
7/25/1989	207	Landsat 4 TM
8/19/1989	231	Landsat 5 TM
8/27/1989	239	Landsat 4 TM
9/4/1989	247	Landsat 5 TM
9/12/1988	255	Landsat 4 TM

isons, atmospherically corrected satellite-based reflectances were compared to the ground data. This study also allowed a preliminary investigation of two of the three new EO-1 bands, band 4p (0.845–0.890 μm) and 5p (1.20–1.30 μm), for agricultural applications.

II. STUDY SITE, MATERIALS AND METHODS

A. Study Sites

Two locations were targeted where extensive ground data were available, the Maricopa Agriculture Center (MAC), owned and managed by the University of Arizona, and the U.S. Department of Agriculture (USDA) Walnut Gulch Experimental Watershed (WGEW) in southeastern Arizona. MAC is located about 48 km southwest of Phoenix, Arizona in an extensively irrigated agricultural region, and is composed of large fields (up to 0.3 × 1.6 km) used for demonstrating new farming techniques on a production scale. WGEW has been instrumented and studied for nearly 50 years by the Southwest Watershed Research Center (SWRC) in Tucson, an entity of the USDA Agricultural Research Service (ARS). The WGEW encompasses 150 km^2 and is representative of approximately 60 million ha of brush- and grass-covered rangeland found throughout the semiarid southwestern United States [7].

B. Landsat-4 TM and Landsat-5 TM Dataset

The dataset for this comparison was comprised of four Landsat-4 TM images and five Landsat-5 TM images acquired in 1989 at MAC (Table I). This dataset was chosen to encompass a cotton-growing season with alternating Landsat-4 and Landsat-5 scenes. Thus, the data could be expected to follow a known trend associated with cotton growth at MAC [5] defined by decreasing surface reflectance (ρ) in the visible bands (bands 1–3) and increasing ρ in the near-infrared band (band 4).

Throughout this cotton-growing season, the ρ of a uniform 0.3 × 1.6 km cotton field was measured with a four-band Exotech radiometer deployed on a low-flying aircraft. The Cessna aircraft was flown at 100 m above ground level to avoid atmospheric attenuation of the radiance reflected from the surface. Coincident measurements of a calibrated 0.5 × 0.5 m $BaSO_4$ reference panel were made with a second Exotech radiometer on the ground, which was cross-calibrated with the airborne radiometer and used to compute ρ from the aircraft-based measurements of radiance (a detailed description of measurement protocol was given by Moran *et al.* [4]). Measurements of reflectance for the length of the field were averaged to one value and the image digital numbers (DNs) associated with this location were extracted from the TM images and averaged to a

TABLE II
LIST OF IMAGES USED FOR THE LANDSAT-5 TM–LANDSAT-7 ETM+ ANALYSIS

Date	DOY	Sensor	Location
3/20/1985	79	Landsat 5 TM	Maricopa
7/23/1985	204	Landsat 5 TM	Maricopa
8/9/1985	220	Landsat 5 TM	Maricopa
10/27/1985	300	Landsat 5 TM	Maricopa
4/21/1986	111	Landsat 5 TM	Maricopa
6/24/1986	175	Landsat 5 TM	Maricopa
5/31/1989	151	Landsat 5 TM	Maricopa
4/23/1992	114	Landsat 5 TM	Walnut Gulch
6/10/1992	162	Landsat 5 TM	Walnut Gulch
7/12/1992	194	Landsat 5 TM	Walnut Gulch
9/30/1992	274	Landsat 5 TM	Walnut Gulch
11/1/1992	306	Landsat 5 TM	Walnut Gulch
11/17/1992	322	Landsat 5 TM	Walnut Gulch
9/24/1999	267	Landsat 7 ETM+	Maricopa
9/26/1999	269	Landsat 7 ETM+	Walnut Gulch
7/26/2000	208	Landsat 7 ETM+	Walnut Gulch
9/12/2000	256	Landsat 7 ETM+	Walnut Gulch
9/26/2000	270	Landsat 7 ETM+	Maricopa
9/28/2000	272	Landsat 7 ETM+	Walnut Gulch
4/22/2001	112	Landsat 7 ETM+	Maricopa
5/24/2001	144	Landsat 7 ETM+	Maricopa
5/26/2001	146	Landsat 7 ETM+	Walnut Gulch
7/27/2001	208	Landsat 7 ETM+	Maricopa
8/29/2001	240	Landsat 7 ETM+	Maricopa
9/29/2001	272	Landsat 7 ETM+	Maricopa

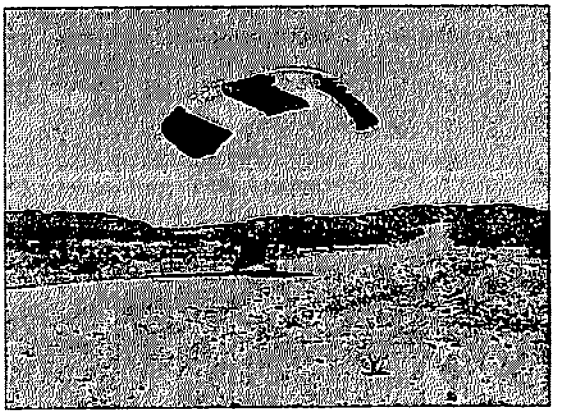

Fig. 1. Powered parachute platform used to deploy a spectrometer for surface reflectance measurements in support of Landsat and EO-1 overpasses.

TABLE III
DATES AND LOCATIONS FOR IMAGE ANALYSIS OF LANDSAT-7 ETM+ AND EO-1 ALI SENSORS

Date	DOY	Location	# of ground data readings
4/22/2001	112	Maricopa	4
5/24/2001	144	Maricopa	4
5/26/2001	146	Walnut Gulch	5
7/27/2001	208	Maricopa	4
8/29/2001	240	Maricopa	2
9/29/2001	272	Maricopa	2
TOTAL			21

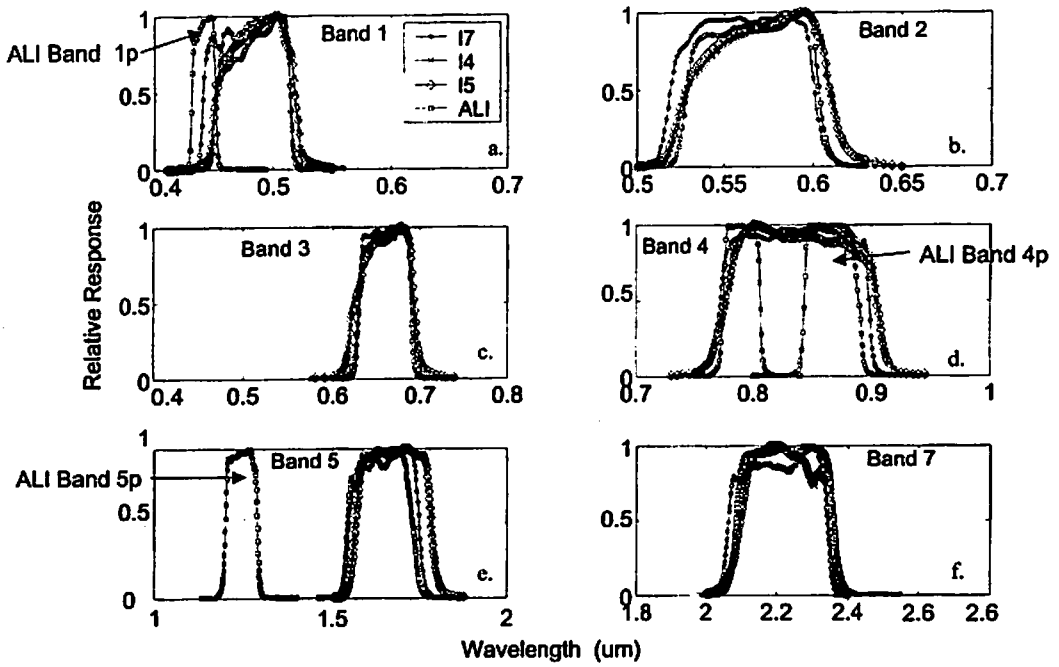

Fig. 2. Response functions for Landsat-4 TM, Landsat-5 TM, Landsat-7 ETM+, and EO-1 ALI

TABLE IV
BAND CHARACTERISTICS OF TM 4, TM 5, ETM+, AND ALI. ASTERICKS INDICATE BANDS USED IN THIS STUDY

TM 4 - TM 5			ETM +			ALI		
	Center	Wavelength		Center	Wavelength		Center	Wavelength
Band	wavelength	range (um)	Band	wavelength	range (um)	Band	wavelength	range (um)
no pan			Pan	0.710	.520-.900	Pan	0.585	0.480-0.690
1*	0.485	0.45-0.52	1*	0.482	0.45-0.52	1*	0.483	0.450-0.515
2*	0.560	0.52-0.60	2*	0.565	0.52-0.60	2*	0.565	0.525-0.605
3*	0.660	0.63-0.69	3*	0.660	0.63-0.69	3*	0.660	0.630-0.690
4*	0.830	0.76-0.90	4*	0.825	0.76-0.90	4*	0.790	0.775-0.805
5	1.650	1.55-1.75	5*	1.650	1.55-1.75	5*	1.650	1.550-1.750
6	11.420	10.40-12.50	6	11.450	10.40-12.50	no thermal		
7	2.215	2.08-2.35	7*	2.220	2.08-2.35	7*	2.215	2.080-2.350
						1p	0.443	0.433-0.453
						4p	0.868	0.845-0.890
						5p	1.250	1.200-1.300

single coincident value. Thus, a dataset of ground-measured ρ was compiled for comparison with ρ retrieved from Landsat-4 and Landsat-5 TM DNs throughout the growing season.

The *refined empirical line* (REL) approach, based on the known reflectance of a within-image target and the modeled DN equivalent of zero reflectance [4], was used to retrieve ρ from satellite DNs. Modeled DN at $\rho = 0$ was 50, 15, 10, and 5 for bands 1–4, respectively. For this study, the within-image target was an alfalfa field for which ground-measured ρ was available from the aircraft-based Exotech measurements. With these two sets of DNs and ρ, linear regression equations were developed to convert the image DN to ρ on each date.

C. Landsat-5 TM and Landsat-7 ETM+ Dataset

Twelve Landsat-5 TM and 13 Landsat-7 ETM+ images were analyzed in this study. More than one target was analyzed for several images for a total of 38 targets, 19 for each platform. Landsat-5 TM images were acquired from 1985 to 1992 and Landsat-7 ETM + images were acquired from 1999 to 2001 (Table II). This dataset was chosen because a Reagan solar radiometer had been deployed to measure atmospheric optical depth during the overpass on each date. The Reagan radiometer, built by engineers at the University of Arizona, measured optical depths at ten different wavelengths to determine molecular optical depth, aerosol optical depth and ozone optical depth. One other parameter necessary for characterizing the atmosphere, the Junge parameter, was also derived from the solar radiometer data (a detailed description of this process was given by Biggar *et al.* [1]).

These atmospheric measurements were used as input to the Gauss–Seidel radiative transfer model (RTM) to define the relationship between surface reflectance and at-sensor radiance.

TABLE V
MAD BETWEEN REFLECTANCES FROM 16 TARGETS CALCULATED FROM RESPONSE CURVES OF LISTED SENSOR PAIRS. TARGETS ARE FROM WALNUT GULCH AND MARCIOPA

Band	TM4 - TM5	TM5 - ETM+	ETM+ - ALI
1	<0.0001	0.0022	0.0015
2	0.0003	0.0049	0.0031
3	0.0002	0.0004	0.0004
4	0.0003	0.0009	0.0059
5	0.0002	0.0009	0.0001
7	<0.0001	0.0011	0.0016

This relationship was used to derive a predicted reflectance at a location in the satellite image where surface reflectance had been measured (a detailed description of this process was given by Thome [8]). Comparing the ground-measured ρ and satellite-retrieved ρ across platforms allowed for an independent test of sensor continuity.

Surface reflectance measurements were made during each overpass using sensors mounted on three different platforms: yoke, aircraft, and powered parachute (Fig. 1). For some overpasses, a four-band Exotech radiometer was mounted on a backpack-type yoke and the operator walked over a 120 × 480 m grid within a uniform field or grassland. Frequent measurements over a calibrated 0.5 × 0.5 m $BaSO_4$ reference panel were used to retrieve surface reflectance (ρ) from the Exotech-measured radiance. The aircraft-based approach was described in the previous subsection. The advantage of aircraft over yoke-based deployment was the ability to measure a greater number of radiometrically different targets in a short time. For the most recent images, the sensor was upgraded from an Exotech to an Analytical Spectral Device (ASD) full-spectrum (FR) hyperspectral spectrometer and the platform was changed from a Cessna aircraft to a powered parachute. In addition, the $BaSO_4$ reference plate was replaced with a more stable pressed Halon plate. The powered parachute is similar to an ultralight but uses a relatively narrow parachute instead of a fixed wing (Fig. 1). This platform was significantly less expensive than an aircraft, required only 30–100 m for takeoff, and used nearby roads for takeoff and landing. For large, uniform targets, the measurements of ρ made with the sensors aboard the aircraft and powered parachute compared to within 0.005 of coincident yoke-based measurements (results not presented here).

Reflectances measured with airborne sensors over designated, uniform MAC fields and WGEW grasslands were extracted and averaged to characterize the reflectance of large targets. The DN associated with these ground locations were extracted from the Landsat TM images, resulting in a set of spatially and temporally coincident ground- and satellite-based data for comparison of satellite-retrieved and ground-measured ρ.

D. Landsat-7 ETM+ and EO-1 ALI Dataset

During the 2001 and 2002 measurement periods, we acquired six coincident (acquired within less than one minute) Landsat-7 ETM+ and EO-1 ALI images at our two study sites. Images were acquired on five dates at MAC and one date at WGEW with cloud-free sky conditions in all cases. As with the Landsat-5 TM, Landsat-7 ETM + comparison, atmospheric optical depths were measured during each overpass and a RTM was used to retrieve surface reflectance from at-satellite radiance. Note that all images used in all studies were ordered from USGS Eros Data Center (EDC) and were radiometrically corrected to Level 1. Calibration coefficients for the Landsat images were taken from the header files. Calibration coefficients from NASA dated December 2001 were used for the ALI images.

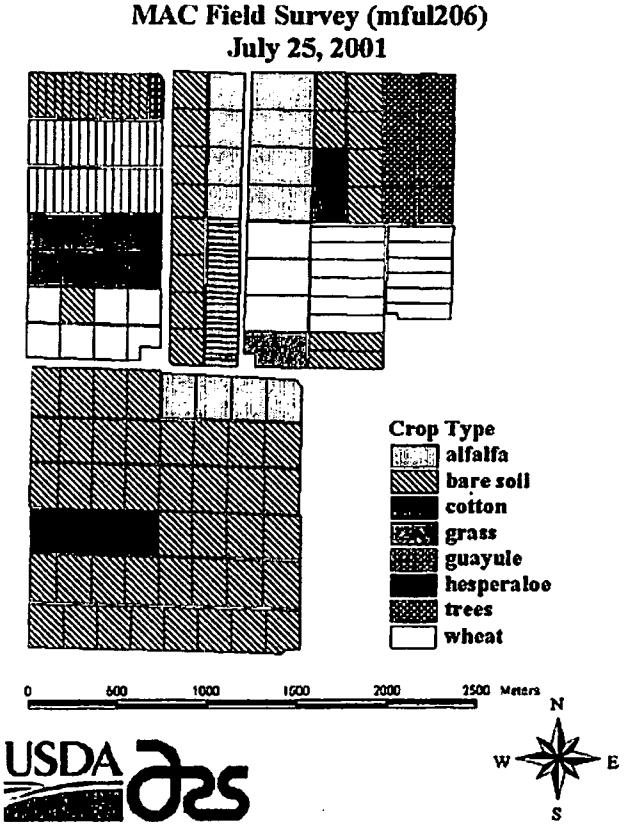

Fig. 3. Example of map produced using information from a MAC field survey.

For field reconnaissance, the powered parachute was deployed with the ASD FR spectrometer. This approach allowed us to analyze 21 different targets using only six images (Tables III and XII). The ALI sensor contains spectral bands that are quite similar to ETM+ bands except for ETM+ band 4, where there are two narrower ALI bands that occur within the ETM+ band 4 [Fig. 2(d)]. Because our surface reflectance measurements for ETM+ and ALI were taken with an ASD FR, we were able to integrate our hyperspectral ground-based measurements to simulate both ETM+ and ALI spectral bands. Note that for this study, we compared ETM+ band 4 with ALI band 4, rather than ALI band 4p.

E. Band Response Function Comparison

Although, equivilant bands between the four sensors being compared are similar, the spectral characteristics of equivilant bands does vary slightly (Table IV, Fig. 2). Before proceeding to analyze equivilant bands from different satellite sensors it is neccesarry to see how the different response functions of the bands affect the data. The first step in this analysis was

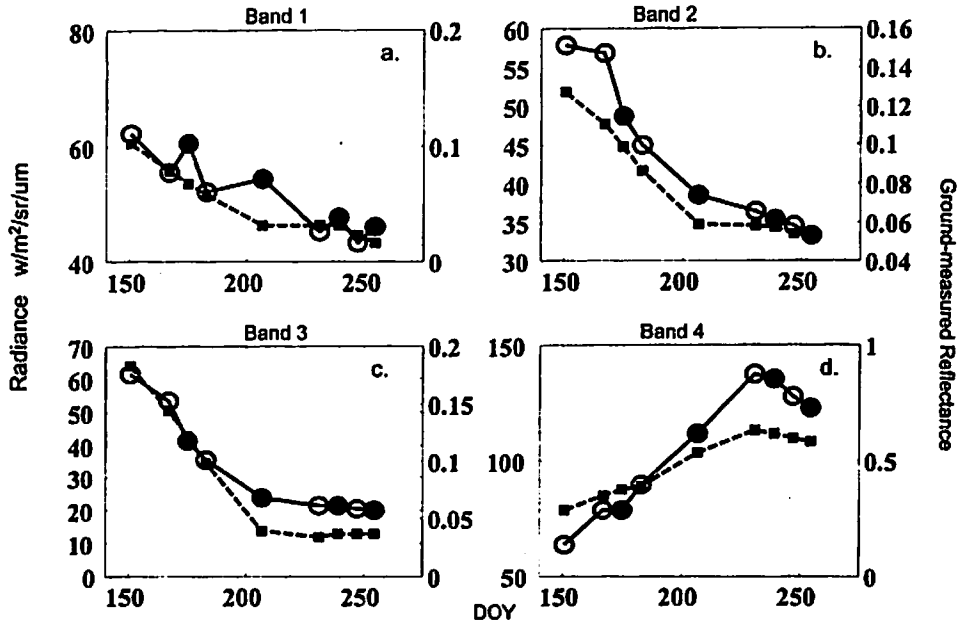

Fig. 4. Radiance and ground-measured reflectance for Landsat-4 TM and Landsat-5 TM for a cotton field at MAC in 1989. The dashed line represents the surface reflectance measured with ground-based sensors, and the solid line represents the radiance retrieved from the sensor. Closed circles represent Landsat-4 TM radiance, and open circles represent Landsat-5 TM radiance.

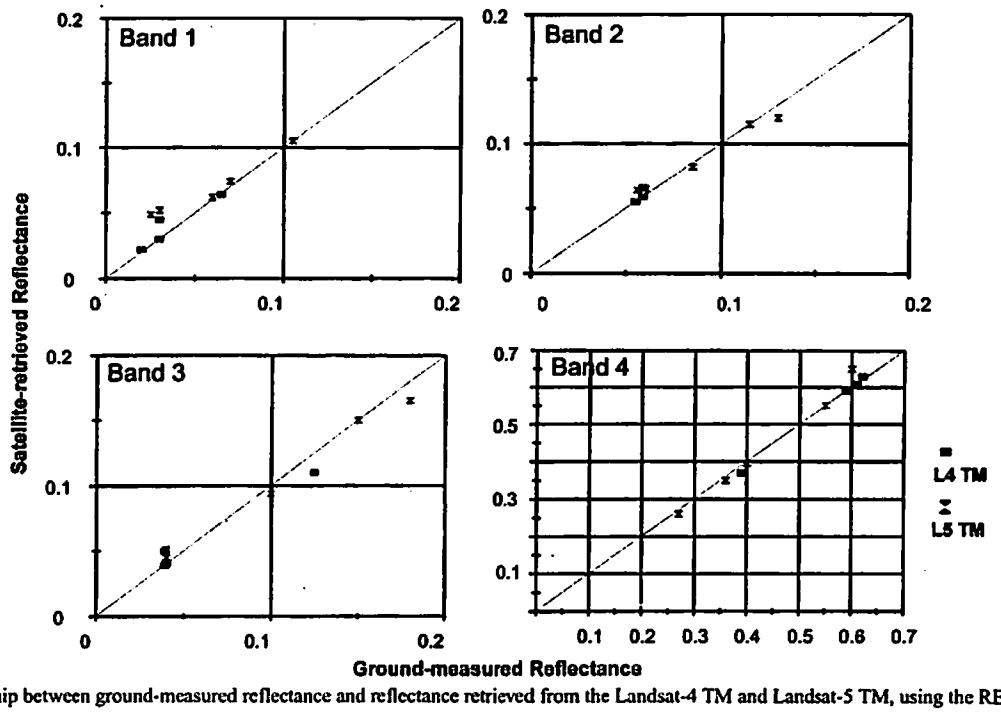

Fig. 5. Relationship between ground-measured reflectance and reflectance retrieved from the Landsat-4 TM and Landsat-5 TM, using the REL method.

TABLE VI
RMSE FOR GROUND REFLECTANCE AND REFLECTANCE DERIVED USING THE REL METHOD FOR LANDSAT-4 TM AND LANDSAT-5 TM SENSORS

Sensor	Band 1	Band 2	Band 3	Band 4
Landsat 4 TM	0.008	0.006	0.009	0.011
Landsat 5 TM	0.015	0.006	0.009	0.023

to compare reflectance values of similar sensor bands, using the ASD measurements of ρ of five targets from WGEW on September 28, 2000 and 11 targets from MAC on April 22, 2001. ASD measurements of ρ in 0.001-μm bands were integrated into TM 4, TM 5, ETM+, and ALI spectral bands using the response functions for each band, and the mean absolute difference was calculated for each sensor pair (Table V). As expected, the reflectances for similar bands between the platforms were extremely close with the highest mean absolute difference (MAD) of 0.0063 for the ETM+/ALI sensor pair in band 4. Sensor pair TM4/TM5 had the best relationship with all MADs

below 0.0005. This is to be expected, since Landsat-5 TM was designed to have the same sensor characteristics as Landsat-4 TM. The highest MAD of 0.0059 for the ETM+/ALI sensor pair is also expected, since these two sensors had considerably different response functions [Fig. 2(d)] compared to the other sensor-band pairs. The overall low MADs for all sensor pairs allowed us consider the bands across sensors essentially equivalent for the targets used in this study.

F. Supporting Data

Extensive field surveys of MAC were performed for the days when images were acquired. Crop cover, crop type, moisture conditions, crop conditions, and fallow field conditions were documented for all production fields on the farm. This information was integrated into a geographic information system so that maps of information of interest could be generated (Fig. 3). This information was very useful for analyzing anomalous image and field data.

III. Results

Since the methodology for analyses of different sensors varied, the results are presented two sensors at a time: Landsat-4 TM to Landsat-5 TM, Landsat-5 TM to Landsat ETM, and Landsat-7 ETM+ to EO-1 ALI. The RMSE statistic is used for all sensor comparisons

$$\text{RMSE} = \sqrt{\frac{\sum_{i=1}^{n} (x_i - y_i)^2}{n}} \tag{1}$$

where

x ρ measured by the ground-based sensor;
y ρ retrieved from the satellite sensor;
n number of observations.

The sensor pair analysis is followed by a statistical comparison of data across all sensors. Finally, results from analysis of two of the three new ALI spectral bands (bands 4p and 5p) are presented.

A. Comparision of Landsat-4 TM to Landsat-5 TM

For the cotton field investigated in the Landsat-4 TM to Landsat-5 TM comparison, ground-based reflectance measurements showed a continuous decrease of reflectance in the visible bands and a continuous increase in the near-infrared (Fig. 4). If there was good data continuity between the Landsat-4 TM and Landsat-5 TM, one would expect the satellite-measured radiance values to follow similar continuous trends. Visually, there was a good correlation between the satellite-measured radiance and the ground-measured reflectance over time in TM bands 2–4 [Fig. 4(b)–(d)]. This was not the case for the radiance measured in TM band 1 [Fig. 4(a)]. It is apparent that the Landsat-4 TM radiance was consistently and substantially higher than the Landsat-5 TM radiance measured over the same field. This indicates a calibration error exists between these two sensors for this scene.

Since the REL approach for retrieving ρ from satellite DNs is an empirical image-based method, it does not depend on an accurate sensor calibration, and the radiance differences in TM band 1 [Fig. 4(a)] were not relevant to the comparison of reflectances. Reflectances derived from Landsat-4 and Landsat-5 TM DNs with the REL method were compared to ground-measured ρ throughout the cotton-growing season. The results showed good continuity for ρ values retrieved from the Landsat-4 TM and Landsat-5 TM sensors and good correlation with ground-measured ρ (Fig. 5).

The RMSE between ground reflectance and REL-computed reflectance was calculated for Landsat-4 TM and Landsat-5 TM. For bands 2 and 3, the RMSE for both platforms was the same, and the RMSE for TM bands 1 and 4 was within 0.01 reflectance value between the two sensors (Table VI) indicating very good data continuity.

B. Landsat-5 TM to Landsat-7 ETM+ Comparison

The Landsat-5 TM to Landsat-7 ETM+ comparison was conducted with data acquired over a 17-year period from 1985 to 2000. Overall, there was a good relation between satellite-retrieved ρ from the Landsat-5 TM and Landsat-7 ETM+ sensors

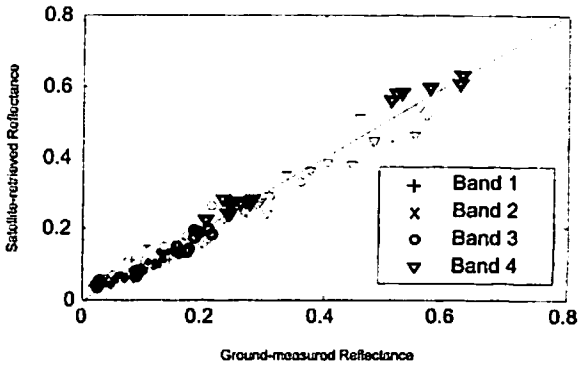

Fig. 6. Relationship between reflectance retrieved from Landsat-5 TM and Landsat-7 ETM+ sensors and associated ground-based reflectance. Bold markers represent Landsat-7 ETM+ and light markers represent Landsat-5 TM.

TABLE VII
RMSE Between Ground-Measured Reflectance and Reflectance Retrieved From Landsat-5 TM and Landsat-7 ETM+ Sensors

Sensor	Band 1	Band 2	Band 3	Band 4
Landsat 5 TM	0.017	0.016	0.022	0.027
Landsat 7 ETM+	0.022	0.018	0.022	0.038

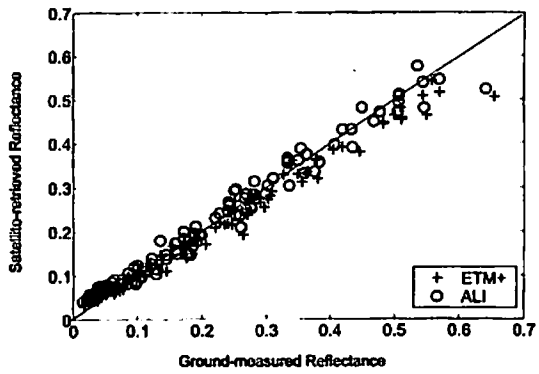

Fig. 7. Relationship between Landsat-7 ETM+ and EO-1 ALI atmospherically corrected satellite-based reflectance and associated ground-based reflectance.

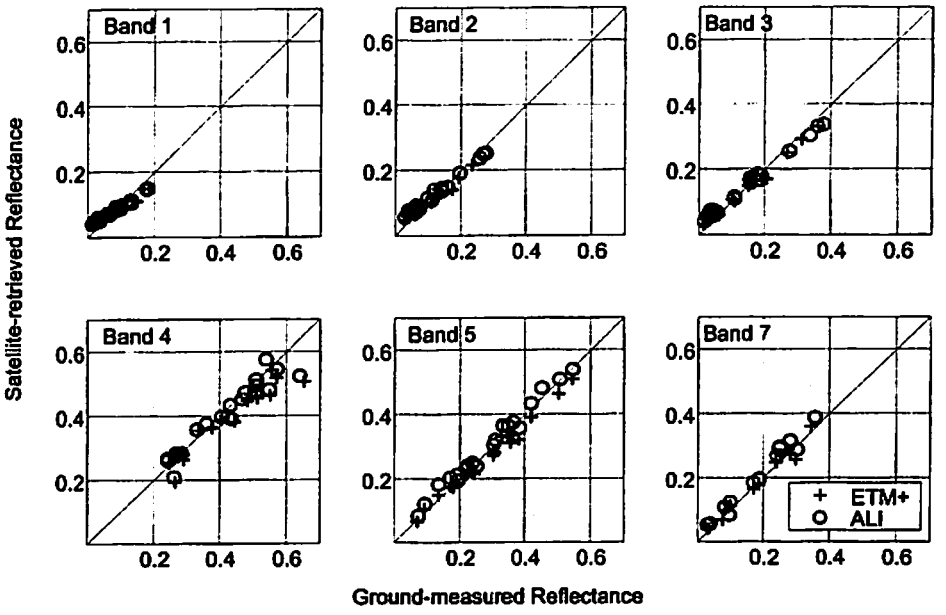

Fig. 8. Relationship between surface reflectances retrieved from Landsat-7 ETM+ and EO-1 ALI, and associated ground-measured reflectance, by band. Circles represent ALI data, and crosses represent ETM+ data.

and the ground-measured ρ (Fig. 6). For all bands and all dates, the RMSE between satellite-retrieved and ground-measured ρ was 0.021 for Landsat-5 TM data, and RMSE was 0.025 for Landsat-7 ETM+ data. The RMSE calculated for each band separately (Table VII) showed similar uncertainty, with RMSE for bands 1–4 ranging from 0.016 (Landsat-5 TM band 2) to 0.038 (Landsat-7 ETM+ band 4). The RMSE values for Landsat-5 TM, bands 5 and 7, were not calculated because ground-measured ρ values for these bands were not available.

C. Landsat-7 ETM+ and EO-1 ALI Comparison

The ground data for the ALI and ETM+ analysis were acquired using an ASD FR spectrometer, which covered a wavelength range from 0.35–2.50 μm. Thus, it was possible to analyze the two shortwave infrared (SWIR) bands along with the visible and near-infrared (NIR) bands, which had not been possible with the Exotech radiometer. Twenty-one data points from six different days at two sites (Table III) were used for our analysis of these two platforms. The procedure for this analysis was similar to our analysis of the Landsat-5 TM and Landsat-7 ETM+ sensors; that is, surface reflectances retrieved from sensor DNs were compared to surface reflectances measured with ground-based sensors (Fig. 7). The RMSE between satellite-retrieved and ground-measured ρ for all bands combined was 0.024 for ALI and 0.028 for ETM+. The RMSE for each band of the two sensors were also computed (see Fig. 8 and Table VIII). The RMSE of ETM+ and ALI band 4, 0.057 and 0.037, respectively, were higher than the RMSE of all other bands, which ranged from 0.013 to 0.032. This was due to the fact that the average reflectance for band 4 was 0.42, whereas average reflectance in all other bands ranged from 0.08 (band 1) to 0.29 (band 5). All RMSE values for equivalent ETM+ and ALI bands were within 0.032 reflectance, indicating very good agreement between the sensors.

TABLE VIII
RMSE BETWEEN ATMOSPHERICALLY CORRECTED SATELLITE-BASED REFLECTANCE AND GROUND REFLECTANCE FOR LANDSAT-7 ETM+ AND ALI

Sensor	Band 1	Band 2	Band 3	Band 4	Band 5	Band 7
Landsat 7 ETM+	0.023	0.024	0.027	0.057	0.032	0.013
EO-1 ALI	0.021	0.020	0.023	0.037	0.020	0.020

Since our comparison of the ETM+ and ALI sensors involved temporally coincident images at the same location, it was possible to make direct comparisons between the sensors (Fig. 9). In this case, the RMSE was computed according to (1), where x = radiances retrieved from ETM+ DNs, y = radiances retrieved from ALI DNs, and n = number of observations [termed RMSE_s to distinguish it from RMSE defined in (1)]. Slope and offset were also computed (Table IX). Although, the linear relationship between radiances was quite good, the slope for the bands ranged from 0.90 to 0.92 for all the bands except for band 4 where the slope was 1.09. Offset for band 4 was negative, and for all the other bands was positive. Because radiance varies so much between bands, the RMSE_s are difficult to compare across bands Therefore, the RMSE_s as a percentage of average radiance for each band was computed. RMSE_s as a percentage of average radiance ranged from 3.0% to 7.6% (Table X) indicating quite good agreement between the sensors. Also, the strong lincarity of the radiance values for both sensors indicates the relative radiometric stability of the sensors throughout the time of this study.

D. Analysis Across All Platforms

The statistical comparisons between sensor pairs reported in previous subsections were based on different measurement and processing methods (see Section II). Thus, the RMSE in one sensor-to-sensor comparison would not be comparable

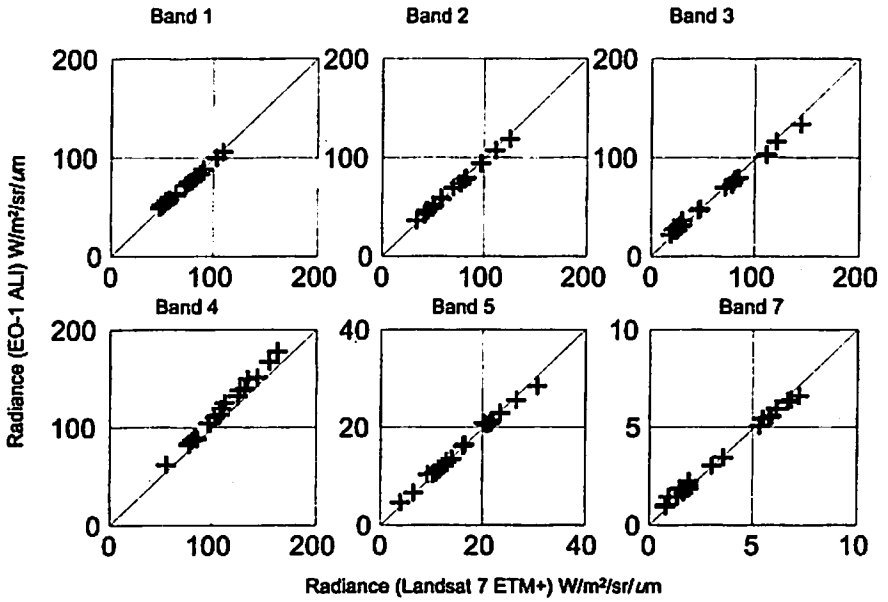

Fig. 9. Relationship between surface reflectances retrieved from Landsat-7 ETM+ and EO-1 ALI, by band.

TABLE IX
LINEAR REGRESSION COEFFICIENTS FOR LANDSAT-7 ETM+ RADIANCES AND EO-1 ALI RADIANCES (IN WATTS PER SQUARE METER PER STERADIAN PER METER). x = ETM+ AND y = ALI

Band	Slope	Offset
1	0.911	5.528
2	0.912	4.655
3	0.901	4.209
4	1.090	-1.875
5	0.928	0.922
7	0.904	0.282

with that of another sensor-to-sensor comparison. To evaluate the data continuity of all four sensors over time and minimize the method-induced differences, the absolute difference of the RMSE between sensor pairs from data in Tables VI–VIII was determined (see Table XI and Fig. 10). Assuming that the RMSE is a similar measure of ground truth accuracy for all the approaches used in this study, the absolute difference of the RMSE between sensor pairs is an unbiased measure of accuracy *across* sensor pairs. Based on that statistic, the highest absolute sensor-to-sensor difference was only 0.020 for band 4 for EO-1 ALI and Landsat-7 ETM+ and differences for all other bands and sensors were less than 0.013 reflectance (Table XI). These results were consistent with the comparisons of reflectances (RMSE) retrieved from ALI and ETM+. The basic conclusion of this analysis is that data continuity across all the Landsat sensors and the ALI sensors is excellent.

E. Evaluation of EO-1 ALI Band 5p

The ALI sensor offers an additional SWIR band called 5p, which ranges from 1.2–1.3 μm. This band was added because it corresponds to a strong atmospheric window in the SWIR spectrum, which might be useful in agriculture and forestry applications [11]. In this study, it was possible to compare the satellite-retrieved ρ values for three ALI SWIR bands for the 21 ground targets at MAC. The simultaneous field surveys of the MAC site near the times of the overpasses provided descriptive data for this qualitative analysis.

The reflectances of the 21 targets measured in ALI bands 5 and 7 showed a wide range of reflectance and a strong correlation between the reflectance measured in ALI bands 5 and 7 (Fig. 11). This was not the case for reflectances retrieved from ALI in band 5p. The vast majority of the retrieved reflectances in ALI band 5p were close to a value of $\rho = 0.40$. The targets that deviated most from $\rho = 0.40$ in ALI band 5p were examined for field data information. Target number 15 had the lowest reflectance and deviated furthest from the cluster. This target was a hesperaloe crop, a yucca-like plant used to make high-quality paper, that had a canopy with much different structural characteristics than any field crop targets in this analysis. Another site with low reflectance was target 3, a pecan orchard that had a canopy with a more complex structure than a common field crop. Target 12 had the same reflectance as target 3 and was mature wheat, characterized by dense heads protruding far above the leaf canopy. The highest reflectance was target 16, which was 5-m-wide alternating strips of wheat stubble and soil. Interestingly, the four targets with the furthest deviation from the cluster were the most structurally heterogeneous targets. The other study sites were cotton or alfalfa crops, weeds, soil, or semiarid grasslands (Table XII).

F. Evaluation of EO-1 ALI Band 4p

The ALI sensor offers two NIR bands that are narrower than ETM+ band 4, but fall within the spectral range of ETM+ band 4 [Fig. 2(d)]. The purpose of the reconfiguration of band 4 in ALI was to avoid the relatively strong water absorption that occurs in the middle of Landsat-7 ETM+ band 4 (0.810–0.840 μm). In our study, we found that columnar water vapor ranged from 1–3 cm, and water vapor absorption reduced satellite-retrieved ρ in the ETM+ band 4 up to 10%. Ground-based measurements of ρ

TABLE X
RMSE, RADIANCE FOR LANDSAT-7 ETM+ AND RADIANCE FOR EO-1 ALI

Sensor	Units	Band 1	Band 2	Band 3	Band 4	Band 5	Band 7
ALI-ETM+	$W/m^2/sr/\mu m$	2.02	2.58	4.02	8.52	0.67	0.25
ALI-ETM+	As a percent of average radiance	3.0%	4.1%	7.2%	7.6%	4.2%	7.1%

TABLE XI
ABSOLUTE DIFFERENCE IN RMSE OF SATELLITE-RETRIEVED REFLECTANCES AND GROUND-BASED REFLECTANCES BETWEEN SENSOR PAIRS

Sensor	Band 1	Band 2	Band 3	Band 4	Band 5	Band 7
TM 5-TM 4	0.007	0.000	0.000	0.012		
ETM+-TM 5	0.005	0.002	0.000	0.011		
ALI-ETM+	0.002	0.004	0.004	0.020	0.012	0.007

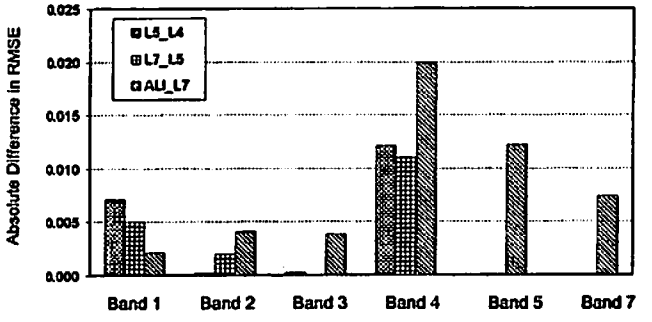

Fig. 10. Difference in RMSE of reflectances retrieved from satellite sensors and ground-measured reflectances between sensor pairs. The legend captions L4, L5, L7, and ALI refer to Landsat-4 TM, Landsat-5 TM, Landsat-7 ETM+, and EO-1 ALI, respectively.

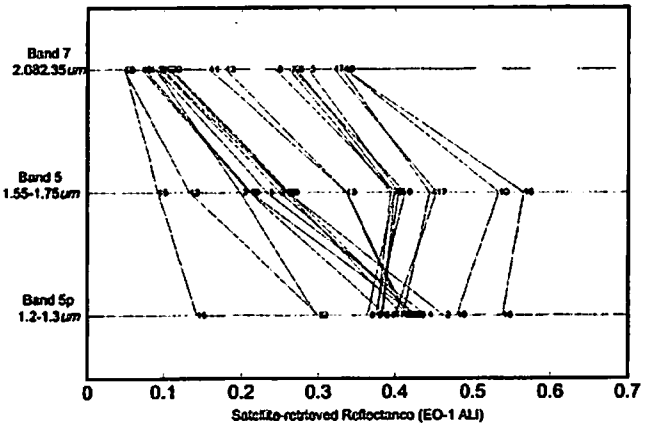

Fig. 11. Reflectances retrieved from EO-1 ALI SWIR spectral bands for all 21 targets. Numbers on the graph correspond to target description in Table IX.

were compared to satellite-retrieved ρ, with and without water vapor correction for these three bands (Table XIII). For ETM+ band 4, accounting for water vapor improved the relationship with ground data; the RMSE was reduced from 0.078 to 0.057. The RMSE for ALI band 4 decreased slightly from 0.053 to 0.041. The RMSE for ALI band 4p was the smallest of all, and there was a negligible difference between the two cases. These results showed that, for our dataset, ALI band 4p was essentially unaffected by atmospheric water absorption.

TABLE XII
DESCRIPTION OF EACH TARGET SITE

Target #	DOY	Target description
1	144	alfalfa
2	144	alfalfa
3	144	pecan orchard
4	144	wheat, senescent
5	146	semi-arid grassland
6	146	semi-arid grassland
7	146	semi-arid grassland
8	146	semi-arid grassland
9	146	semi-arid grassland
10	240	alfalfa wet
11	240	wheat stubble
12	112	wheat
13	112	weeds
14	112	road
15	112	hesperaloe
16	208	wheat senescent
17	208	soil
18	208	cotton
19	208	alfalfa
20	272	alfalfa
21	272	alfalfa

TABLE XIII
RMSE REFLECTANCE RETRIEVED FROM LANDSAT-7 ETM+ BAND, EO-1 ALI BAND 4 AND 4P AND ASSOCIATED GROUND REFLECTANCE. TWO CASES ARE PRESENTED: ATMOSPHERIC CORRECTION WITHOUT WATER VAPOR CORRECTION AND WITH WATER VAPOR CORRECTION

Band	Without water vapor correction	With water vapor correction
ETM+ Band 4	0.078	0.057
ALI Band 4	0.052	0.041
ALI Band 4p	0.037	0.034

In terms of data continuity between ETM+ and ALI, it was demonstrated that ALI band 4 and ETM+ band 4 had very similar reflectance characteristics, at least for a semiarid grassland (Table V). However, when comparing at-satellite radiances between these two bands, caution should be exercised due to the different atmospheric water absorption properties.

IV. Conclusion

Three separate analyses of data continuity were conducted for Landsat-4 to Landsat-5 TM, Landsat-5 TM to Landsat-7 ETM+ and Landsat-7 ETM+ to EO-1 ALI. In all cases, the RMSE [(1)] between satellite-retrieved and ground-measured reflectance were comparable between sensors, and the RMSE was generally within the required accuracy for many applications (Tables VI–VIII). The direct comparison between image pairs of Landsat-7 ETM+ and EO-1 ALI (Table X) showed reasonable comparability with $RMSE_s$ as a percentage of average radiance ranging from 3% (band 1) to 7.6% (band 4). When the RMSE of all sensors were compared (to minimize the effects of different methodologies), the sensors showed excellent data continuity. The absolute differences in RMSE ranged from 0.00 to 0.02 (Table XI).

The qualitative analysis of the new ALI spectral bands (4p and 5p) showed that ALI band 5p provided information that was different from that provided by the ETM+/ALI bands 5 and 7 for agricultural targets (Fig. 11). Further investigation is warranted to determine what distinctive surface characteristics influenced the reflectance in band 5p. The ALI band 4p has the advantage over the ETM+ band 4 and ALI band 4 of being relatively insensitive to water vapor absorption (Table XIII). Furthermore, since the reflectances retrieved from ETM+ band 4, ALI band 4, and ALI band 4p for our 21 agricultural targets were nearly identical (data not shown here), it could be an excellent substitute band for ETM+ band 4 on the next Landsat mission.

This work presented an in-flight analysis of three Landsat sensors and the new ALI sensor. Combined, these four sensors have provided images for the past 20 years, and Landsat-7 ETM+ will continue to provide images for ten more years, if the lifespan of the sensor is similar to that of Landsat-5 TM. This represents a potential data stream of earth images spanning over 30 years. The basic conclusion of this study is that the four sensors can provide excellent data continuity for temporal studies of natural resources. This could represent a new age in which temporal *and* spatial changes in natural resources can be monitored and managed with the use of moderate resolution satellite imagery. Furthurmore, the new technologies put forward by the EO-1 ALI sensor have increased the SNR and improved data quantization [2]. This has been accomplished with no apparent effect on data continuity. In addition, the new NIR and SWIR bands may offer a signal that is less attenuated by the atmosphere (ALI band 4p) and new surface information (ALI band 5p). The EO-1 ALI mission has been successful in testing new technologies for the upcoming Landsat-8 sensor payload.

References

[1] S. F. Biggar, D. I. Gellman, and P. N. Slater, "Improved evaluation of optical depth components from Langley plot data," *Remote Sens. Environ.*, vol. 32, pp. 91–101, 1990.

[2] D. E. Lencioni, C. J. Digenis, W. E. Bicknell, D. R. Hearn, and J. A. Mendenhall, "Design and performance of the EO-1 advanced land imager," in *Proc. SPIE Conf. Sensors, Systems, and Next Generation Satellites III*, Florence, Italy, Sept. 20, 1999.

[3] M. D. Metzler and W. A. Malila, "Characterization and comparison of Landsat-4 and Landsat-5 Thematic Mapper data," *Photogramm. Eng. Remote Sens.*, vol. 51, no. 9, pp. 1315–1330, 1985.

[4] M. S. Moran, R. Bryant, K. Thome, W. Ni, Y. Nouvellon, M. P. Gonzalez-Dugo, J. Qi, and T. R. Clarke, "A refined empirical line approach for reflectance factor retrieval from Landsat-5 and Landsat-7 ETM+," *Remote Sens. Environ.*, vol. 78, pp. 71–82, 2001.

[5] P. R. Pinter Jr, R. J. Anderson, B. A. Kimball, and J. R. Mauney, "Evaluating cotton response to free air carbon dioxide enrichment withcanopy reflectance observations," *Critical Rev. Plant Sci.*, vol. 11, no. 2-3, pp. 241–250, 1992.

[6] J. C. Price, "Calibration comparison for the Landsat 4 and 5 multi-spectral scanners and Thematic Mappers," *Appl. Opt.*, vol. 28, no. 3, pp. 465–471, 1989.

[7] K. J. Renard, L. J. Lande, J. R. Simanton, W. E. Emmerich, J. J. Stone, M. A. Weltz, D. C. Goodrich, D. S. Yakowitz, and D. S., "Agricultural impacts in an arid environment: Walnut gulch studies," *Hydrol. Sci. Technol.*, vol. 9, pp. 145–190, 1993.

[8] K. J. Thome, "Absolute radiometric calibration of Landsat 7 ETM+ using the reflectance-based method," *Remote Sens. Environ.*, vol. 78, pp. 27–38, 2001.

[9] J. E. Vogelmann, M. J. Choate, D. Helder, J. W. Merchant, and H. Bulley, "Effects of Landsat Thematic Mapper radiometric and geometric calibrations on selected land cover analyses," in *Proc. Pecora 14/Land Satellite Information III Conf.*, Dec. 6–10, 1999.

[10] J. E. Vogelmann, D. Helder, R. Morfitt, M. J. Choate, J. W. Merchant, and H. Bulley, "Effects of Landsat 5 Thematic Mapper and Landsat 7 enhanced Thematic Mapper plus radiometric and geometric calibrations and corrections on landscape characterization," *Remote Sens. Environ*, vol. 78, pp. 55–70, 2001.

[11] J. Irons, private communication.

Ross Bryant received the B.A. degree in geology from Colorado College, Colorado Springs, and the M.S. degree in soil and water science from the University of Arizona, Tucson.

He is currently a Remote Sensing Scientist with for the U.S. Department of Agriculture, Agriculture Research Service, Tucson, AZ. He has spent two summers as a mining geologist in Colorado before traveling the United States and the South Pacific for a year. Upon returning to the United States, he spent several years in the social services and then returned to graduate school. After graduate studies, he worked for the University of Arizona on global change issues before being employed by the U.S. Department of Agriculture.

M. Susan Moran received the B.S. degree from San Diego State University, San Diego, CA, and the M.S. degree from the University of California, Santa Barbara, both in geography, in 1976 and 1982, respectively, and the Ph.D. degree in soil and water science from the University of Arizona, Tucson, in 1990.

She is currently a Research Leader with the U.S. Department of Agriculture, Agriculture Research Service, Southwest Watershed Research Center, Tucson, AZ. Her research interests focus on estimation of soil moisture and plant stress utilizing a combination of models and remote sensing techniques.

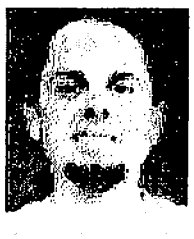

Stephen A. McElroy received the B.A. degree in international affairs from the University of Cincinnati, Cincinnati, OH, the M.A. degree in Latin American studies from the University of Arizona, Tucson, and the Ph.D. degree in geography from San Diego State University, San Diego, CA, in 1991, 1994, and 1999, respectively.

He is currently a Remote Sensing and GIS Research Specialist with the U.S. Department of Agriculture, Agriculture Research Service, Southwest Watershed Research Center, Tucson, AZ and is an Adjunct Professor of geography at Pima Community College, Tucson, AZ.

Chandra D. Holifield received the B.S. degree in plant and soil science in 1998 and the M.S. degree in plant science from the University of Arizona, Tucson, in 2000, where she conducted a comparison of modern and obsolete cotton cultivars for irrigated production in Arizona.

She is currently a Support Scientist with the U.S. Department of Agriculture (USDA), Agriculture Research Service (ARS), Tucson, AZ, and is exploring the use of remote sensing for rangeland management.

Ms. Holifield received a USDA/1890 National Scholar Award while a senior in high school, which resulted in a full scholarship to Virginia State University, Petersburg.

Kurtis J. Thome received the B.S. degree in meteorology from Texas A&M University, College Station, and the M.S. and Ph.D. degrees in atmospheric sciences from the University of Arizona, Tucson.

He is currently an Associate Professor of optical sciences at the University of Arizona, where he is the head of the Remote Sensing Group. He has served as a member of the Landsat-7, ASTER, and MODIS science teams. His current research is focused on the vicarious calibration of earth-imaging sensors and related studies in atmospheric remote sensing, radiative transfer, and satellite atmospheric correction

Tomoaki Miura (M'03) received the M.S. degree in resource management from the University of Nevada, Reno, in 1996, and the Ph.D. degree in soil, water, and environmental science from the University of Arizona, Tucson, in 2000.

He is currently an Associate Research Scientist with the Terrestrial Biophysics and Remote Sensing Laboratory, University of Arizona. He is also a Science Validation Team Member of the EO-1 instrument and is also involved in the Airborne Science Project within the Brazil-led Large-scale Biosphere-Atmosphere Experiment in the Amazon. His research interests include sensor calibration, error/uncertainty analyses, and hyperspectral remote sensing.

Stuart F. Biggar received the B.S. and M.S. degrees in physics from the United States Air Force Academy, Colorado Springs, CO, and The Ohio State University, Columbus, respectively. He received the M.S. and Ph.D. degrees in optical sciences from the Optical Sciences Center, University of Arizona, Tucson.

He is currently a Research Professor of optical sciences at the University of Arizona, working in the Remote Sensing Group. His current research includes radiometry, radiometric calibration of optical systems, diffuse reflectance measurements, and vicarious calibration of optical sensors.